COMMUNICATION

An Apoferritin-based Drug Delivery System for the Tyrosine Kinase Inhibitor Gefitinib

*Anchala I. Kuruppu, Lei Zhang, Hilary Collins, Lyudmila Turyanska, Neil R. Thomas, and Tracey D. Bradshaw**

Development of a tumor-specific drug delivery system is challenging and depends immensely on the carrier. Currently various approaches are considered to develop efficient drug delivery systems.[1,2] Leaky vasculature, associated with sustained tumor angiogenesis together with tumor-associated poor lymphatic drainage can enhance passive targeting of nanoparticles (NPs) to malignant tissue resulting in the enhanced permeability retention effect.[3,4] Nanoparticulate drug formulations, exploiting this feature of the tumor microenvironment, can be used to deliver chemotherapeutic agents to tumor target sites thereby increasing the therapeutic effect while minimizing systemic toxicities.[5] When selecting a delivery system a major consideration is controlled release of the drug to the target site at a therapeutically optimal rate.[1,6]

Human ferritin is an ideal drug delivery carrier due to the nanoscale structure, and biocompatible, biodegradable, stable, nontoxic properties.[2,7,8] Ferritin consists of an apoferritin (AFt) protein cage and an iron core, and prevents accumulation of toxic levels of free iron in cells. AFt is composed of 24 subunits arranged into a 12 nm diameter cage with an internal 8 nm cavity. AFt is comprised of heavy (H) and light (L) chains which are highly homologous but functionally distinct. The AFt cage has 14 channels, each 3–4 Å in diameter, to allow exchange of cargo between the protein cage interior and exterior environments. Among the 14 channels, eight are hydrophilic and six are hydrophobic.[6,7,9] Also, the AFt cage can disassemble into subunits at low pH (<pH 4.0) allowing release of cargo, and reassemble at higher pH (>pH 5.0).[5] Ferritin circulates and binds to a variety of cell types, however, specific binding to cells has been seen only for H-ferritins.[10] Ferritin binding sites and endocytosis of ferritin have been found in neoplastic cells,[11] and were associated with membrane-specific transferrin receptors (TfR) that are highly expressed in many cancers[12] including breast and brain cancer cells.[12,13] The unique architecture of AFt provides two interfaces: the outer surface of AFt can be modified chemically or genetically with functional motifs[14] and the internal cavity can be used to encapsulate pharmaceutical agents such as anticancer drugs, magnetic resonance imaging (MRI), and fluorescent imaging agents.[6,9,15,16] Recently, selective targeting and cargo delivery with heavy chain apoferritin (H-AFt) was demonstrated both in vitro[17] and in vivo.[18]

Gefitinib ("Iressa," ZD1839) is an orally active, epidermal growth factor receptor (EGFR) tyrosine kinase inhibitor.[19] This receptor family comprises four homologous receptors: EGFR (ErbB1/HER1), HER2 (ErbB2), HER3 (ErbB3), and HER4 (ErbB4), which have an extracellular ligand binding domain, a single hydrophobic trans-membrane domain and a cytoplasmic tyrosine kinase domain. These receptors are activated by either homo- or heterodimerization upon ligand binding resulting in phosphorylation of specific tyrosine residues.[20,21] The overexpression of EGFR and HER2 in breast cancer, is associated with poor prognoses.[20,22,23] Gefitinib is used for treatment of EGFR and HER2 overexpressing breast cancers.[24,25] However, the therapeutic window of this drug is drastically narrowed by poor bioavailability, acquired resistance due to insufficient or ineffective cellular uptake and systemic toxicity resulting from interactions between drug and healthy tissue.[19,26] Also, orally administered Gefitinib is taken up extensively by human serum albumin and hence other delivery systems such as liposomes have been investigated.[27] Development of a selective targeted delivery system would improve efficiency of Gefitinib treatment.

Herein, we report the use of human H-AFt as a delivery cage for Gefitinib to improve drug selectivity for HER2 overexpressing cells. The H-AFt-encapsulated-Gefitinib (H-AFt/Gefitinib) nanocomposite has potent and enhanced antitumor activity against the HER2 overexpressing SKBR3 breast cancer cell line ($GI_{50} = 0.52 \times 10^{-6}$ M) compared to Gefitinib alone ($GI_{50} = 1.66 \times 10^{-6}$ M; **Table 1**). Enhanced drug efficacy is achieved through sustained controlled drug release from the H-AFt cavity. In contrast, H-AFt-encapsulated-Gefitinib treatment of MDA-MB-231 breast cancer cell line, which does not express HER2, has shown decreased uptake of Gefitinib compared to treatment with unencapsulated drug. These results expose prospects for utilization of H-AFt as a carrier for targeted delivery of anticancer drugs to HER2 overexpressing tumors.

For efficient entrapment of any drug into a delivery system, consideration of physical properties of both the drug and delivery system is important. Gefitinib is a hydrophobic drug and H-AFt has six hydrophobic channels allowing the drug molecules to enter the H-AFt cavity by passive diffusion

A. I. Kuruppu, Dr. H. Collins, Dr. T. D. Bradshaw
Centre for Biomolecular Sciences
School of Pharmacy
The University of Nottingham
Nottingham NG7 2RD, UK
E-mail: Tracey.Bradshaw@nottingham.ac.uk
Dr. L. Zhang, Prof. N. R. Thomas
Centre for Biomolecular Sciences
School of Chemistry
The University of Nottingham
Nottingham NG7 2RD, UK
Dr. L. Turyanska
School of Physics and Astronomy
The University of Nottingham
Nottingham NG7 2RD, UK

The copyright line of this paper was changed 8 June 2016 after initial publication.

DOI: 10.1002/adhm.201500389

Table 1. Effect of Gefitinib, H-AFt-encapsulated-Gefitinib, and H-AFt on growth of SKBR3 and MDA-MB-231 cells. It should be noted that the GI_{50} values for H-AFt-encapsulated-Gefitinib refer to encapsulated Gefitinib concentration; the amount of Gefitinib encapsulated per H-AFt cage impacts material potency and merits further detailed studies.

	Mean GI_{50} value ± SE [μM]					
	Gefitinib		H-AFt-encapsulated-Gefitinib		H-AFt	
Cell line	72 h	120 h	72 h	120 h	72 h	120 h
SKBR3	0.94 ± 0.49	1.66 ± 0.79	1.44 ± 0.49	0.52 ± 0.17	4.84 ± 3.43	5.50 ± 3.81
MDA-MB-231	21.80 ± 0.52	19.56 ± 0.64	>25	>25	16.47 ± 0.98	19.85 ± 0.15

during mixing of the drug with the protein (**Figure 1**a).[28] Gefitinib has low solubility in aqueous buffers[29] and was first dissolved in dimethylsulfoxide (DMSO) and then diluted with phosphate buffered saline (PBS) at pH 7.2. This 1×10^{-3} M aqueous solution of Gefitinib was mixed with H-AFt. The lateral dimensions of Gefitinib are ≤0.3 nm, allowing Gefitinib intake through six hydrophobic channels by diffusion. The resulting solution was exhaustively dialyzed and centrifuged at high speed to remove any unencapsulated Gefitinib and any impurities. The encapsulation of Gefitinib was confirmed by UV spectrophotoscopy. Absorbance of Gefitinib was analyzed at 250 nm and the encapsulation efficiency (EE) was quantified according to the Beer–Lambert law to be ≈55%.

Mass spectrometry measures the mass to charge ratio and can be used to determine the purity and the molar mass of the particles.[30] Matrix-enriched laser desorption ionization (MALDI) studies revealed high intensity peaks for H-AFt and Gefitinib which indicates high abundance of the drug and the protein in the mixture corresponding to a H-AFt molecular weight (M_W) of 24.71 kDa and Gefitinib M_W of 442.6 Da, comparable to the expected values (S1, Supporting Information). Protein determination by Bradford assay revealed 1.25 mg H-AFt per ml—equivalent to 50.6×10^{-6} M. UV spectrophotometry determined a ratio of 605×10^{-6} M Gefitinib/50.6×10^{-6} M H-AFt indicating >10 molecules of Gefitinib per H-AFt cavity. Further evidence of Gefitinib encapsulation within H-AFt was provided by flow cytometry analysis (Section S1, Supporting Information).

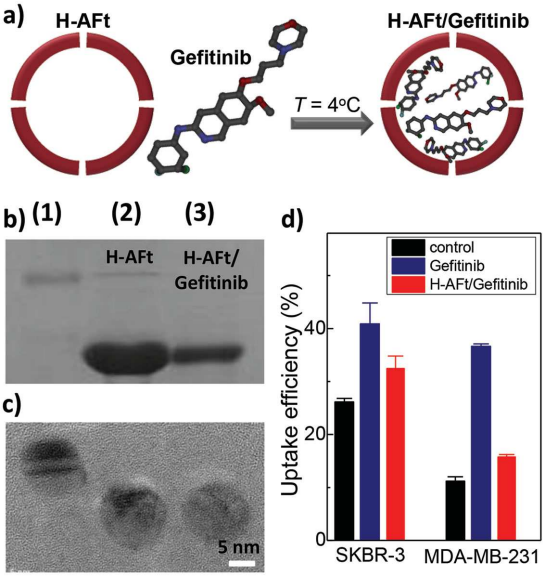

Figure 1. a) Schematic representation of preparation of H-AFt-encapsulated Gefitinib encapsulated NPs. b) PAGE- 1) Marker 2) H-AFt 3) H-AFt-encapsulated-Gefitinib. c) TEM Images of H-AFt-encapsulated Gefitinib confirming the size of the NPs. d) Mean fluorescence uptake by SKBR3 and MDA-MB-231 cells using flow cytometry. Mean and SD of 3 independent trials ($n = 2$ per trial).

The stability and the structural integrity of H-AFt-encapsulated-Gefitinib were confirmed by polyacrylamide gel electrophoresis (PAGE) and transmission electron microscopy (TEM). PAGE profile of H-AFt-encapsulated-Gefitinib revealed a band similar to that of H-AFt only, at $M_W \approx 24.7$ kDa (Figure 1b). This indicates that the AFt protein structure and charge remain unchanged after encapsulation of Gefitinib. TEM images (Figure 1c) show intact H-AFt shells with an outer diameter of 12.5 ± 0.46 nm, and confirm that the H-AFt-encapsulated-Gefitinib retains the spherical shape and the size expected for H-AFt. The electron density of Gefitinib molecules is similar to that of H-AFt, hence there was insufficient contrast to resolve encapsulated Gefitinib in TEM.

In vitro effects of H-AFt-encapsulated-Gefitinib were assessed using the HER2 overexpressing SKBR3 cell line that expresses low levels of EGFR. As a negative control MDA-MB-231 cell line was used which does not express HER2 but expresses high levels of EGFR.[24]

Cellular internalization of H-AFt-encapsulated-Gefitinib was observed by confocal microscopy and compared to that of Gefitinib. SKBR3 and MDA-MB-231 cells were treated with H-AFt-encapsulated-Gefitinib, Gefitinib, and H-AFt (5×10^{-6} M) for 24 h (**Figure 2**; Section S2, Supporting Information). The fluorescence of Gefitinib is environmentally sensitive: peak excitation and emission depends upon environment polarity and is intense in nonpolar solvents.[31] This property has allowed cellular uptake and distribution studies to be performed. Intracellular Gefitinib was evident from the bright fluorescence observed within the cytoplasm of SKBR3 cells treated with H-AFt-encapsulated-Gefitinib. Cytoplasmic Gefitinib fluorescence was punctuate consistent with localization in acidic lysosomes and endosomes within these cells.[31] SKBR3 cells treated with H-AFt alone appeared to be identical to control cells and did not show fluorescence. Also MDA-MB-231 cells treated with H-AFt-encapsulated-Gefitinib did not show bright fluorescence compared to MDA-MB-231 cells treated with Gefitinib indicating uptake suppression.

The cellular uptake of H-AFt-encapsulated-Gefitinib was quantified using flow cytometry. SKBR3 and MDA-MB-231 cells were treated with H-AFt-encapsulated-Gefitinib or Gefitinib (5×10^{-6} M) for 24 h and compared to control. Mean fluorescence was used as a measure of Gefitinib uptake by the cells

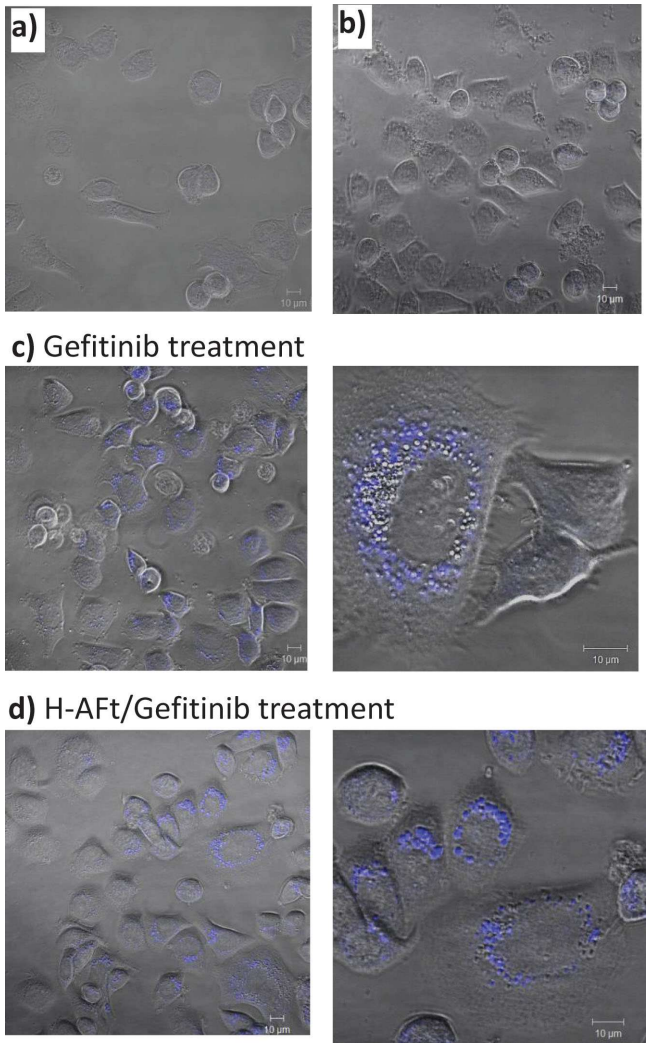

Figure 2. Confocal microscopy images of SKBR3 cells demonstrating cellular uptake of Gefitinib after 24 h exposure of cells to: a) control, b) H-AFt, c) Gefitinib, d) H-AFt-encapsulated-Gefitinib. Representative images of 3 independent trials are shown ($n = 2$ per trial).

(Figure 1d). Significant uptake by SKBR3 and MDA-MB-231 cells were measured for Gefitinib. Uptake of H-AFt-encapsulated-Gefitinib by SKBR3 cells was also significant; however uptake of H-AFt-encapsulated-Gefitinib by MDA-MB-231 cells was not significant compared to control. Thus, qualitative observations of confocal microscopy were corroborated by flow cytometry analyses, and demonstrate successful internalization of H-AFt-encapsulated-Gefitinib by HER2 overexpressing SKBR3 cells.

In order to study *in vitro* antitumor activity of H-AFt-encapsulated-Gefitinib, cells were incubated with H-AFt-encapsulated-Gefitinib, Gefitinib, and H-AFt for 72 h and growth inhibition was determined by MTT assay (Table 1; **Figure 3**a,b; Section S3, Supporting Information). Interestingly, the SKBR3 cell line was sensitive to both Gefitinib ($GI_{50} = 0.94 \pm 0.49 \times 10^{-6}$ M) and H-AFt-encapsulated-Gefitinib ($GI_{50} = 1.44 \pm 0.49 \times 10^{-6}$ M). However, the reduced potency of H-AFt-encapsulated-Gefitinib compared to Gefitinib alone implies that encapsulated Gefitinib may require time to be released from the H-AFt cavity as it is processed by endosome and lysosome systems with a local pH gradually reducing.[31] Conversely the MDA-MB-231 cell line demonstrated significantly reduced sensitivity to both Gefitinib ($GI_{50} = 21.80 \pm 0.52 \times 10^{-6}$ M) and H-AFt-encapsulated-Gefitinib ($GI_{50} > 25 \times 10^{-6}$ M).

Although Gefitinib is an EGFR tyrosine kinase inhibitor, no correlation was observed between EGFR expression and sensitivity of cells. Gefitinib activity requires a phosphorylated (active) form of EGFR whereas MDA-MB-231 cells express nonphosphorylated EGFR and hence are not sensitive to this drug.[24] On the other hand, cancer cells that express low levels of EGFR together with overexpression of HER2 are sensitive to this drug and indeed, high sensitivity of SKBR3 cells to Gefitinib was observed.[24,25] HER2 remains the preferred dimerization partner of other ErbB receptors. Although both homo- and hetero-dimerization activate the EGFR network, heterodimers are found to be more potently mitogenic and HER2 heterodimers generate the strongest biological activity compared to other heterodimers.[20,24,32]

TfR1 is associated with uptake of H-AFt and is more highly expressed in cancer cells compared to normal human cells.[12] It has been found that the expression of TfR1 correlates with tumor stage or cancer progression.[4] Iron is required by many cellular processes such as metabolism and DNA synthesis. TfR1 resides on cell membranes and imports cargo by receptor-mediated endocytosis via clathrin-coated pits.[4,8] Both SKBR3 and MDA-MB-231 cells possess high levels of TfR1[33] which would assist cellular uptake of H-AFt-encapsulated-Gefitinib.[34] The greater SKBR3 growth inhibition by H-AFt compared to MDA-MB-231 implies greater sequestration of H-AFt by SKBR3 cells. Indeed, it has been shown previously that ferritin was not taken up by MDA-MB-231 cells.[35] In this study, the enhanced activity of H-AFt-encapsulated-Gefitinib in HER2 overexpressing cells is also a consequence of Gefitinib inhibition of kinase activity, and therefore EGFR signaling triggered by HER2-EGFR dimerization.

To determine whether a longer exposure time to encapsulated drug would be more effective in cells, MTT assays were performed following 120 h treatment (Table 1, Figure 3c,d). Again the SKBR3 cell line showed greater sensitivity to H-AFt alone compared to MDA-MB-231 cells. Interestingly the GI_{50} value for H-AFt-encapsulated-Gefitinib ($0.52 \pm 0.17 \times 10^{-6}$ M) against the SKBR3 cell line was lower compared to the 72 h assay ($GI_{50} = 1.44 \pm 0.49 \times 10^{-6}$ M) and it was also lower (≈3-fold) than that of Gefitinib after 120 h exposure ($GI_{50} = 1.66 \pm 0.79 \times 10^{-6}$ M). No significant difference was found between the GI_{50} values of Gefitinib alone at 72 and 120 h. It should be noted that at H-AFt-encapsulated-Gefitinib GI_{50} values of 1.44×10^{-6} and 0.52×10^{-6} M, equivalent concentrations of AFt were 0.11×10^{-6} and 0.04×10^{-6} M respectively, concentrations which negligibly impact SKBR3 cellular proliferation. Consistent with results following 72 h exposure, after 120 h exposure, the MDA-MB-231 cell line did not show sensitivity to H-AFt-encapsulated-Gefitinib, $GI_{50} > 25 \times 10^{-6}$ M (equivalent to 2.1×10^{-6} M AFt).

These results demonstrate that drug encapsulation enhances Gefitinib activity in SKBR3 cells and support the hypothesis that the H-AFt cage allows controlled release of drug molecules.

Tumor microenvironments exhibit lower extracellular pH than normal tissues while the intracellular pH of cells within

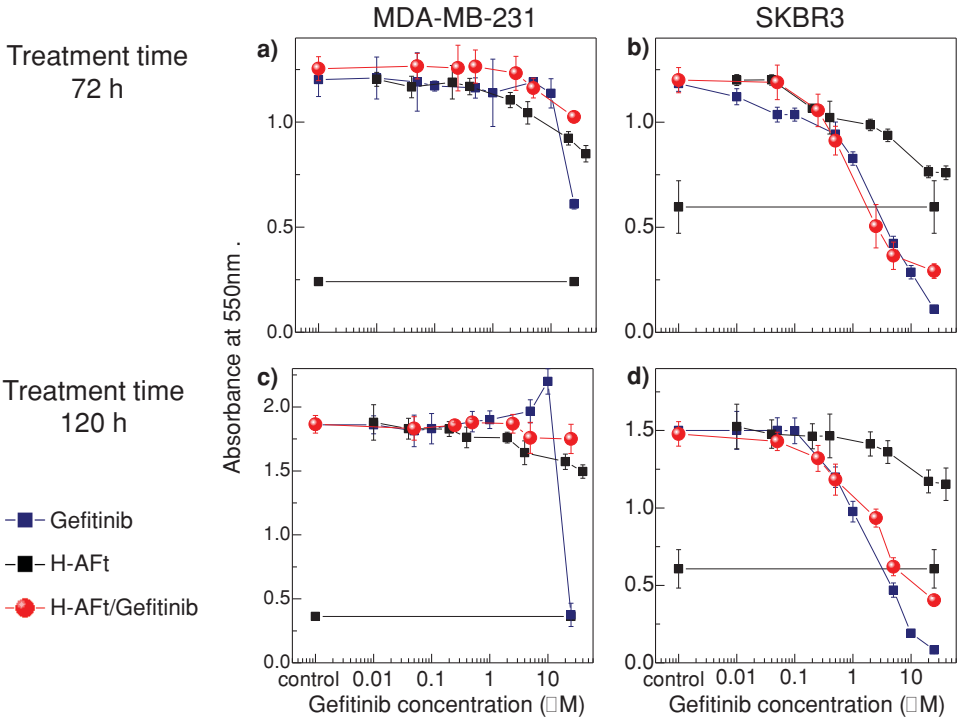

Figure 3. Representative growth inhibitory curves for Gefitinib, H-AFt, and H-AFt-encapsulated-Gefitinib. The concentration of the H-AFt only sample is normalized to the concentration of AFt in H-AFt-encapsulated-Gefitinib. a,c) MDA-MB-231 and b,d) SKBR3 cells were seeded at a density of 2.5×10^3 in 96 well plates at pH 7.5. Following a,b) 72 h or c,d 120 h exposure to test agents, cell growth and viability were determined by MTT assays. Mean and SD of representative experiments of ≥3 independent trials are shown ($n = 8$ per trial).

normal and tumor cells is similar.[5] The overall pH range within a tumor environment is 6.5–7.2 where as normal cells possess a pH range of 7.2–7.4, allowing pH controlled release.[36] Further, the pH-dependent release of cargo could offer additional advantage for applications in stomach cancers, where an acidic environment would enhance drug release from the AFt cavity. Hence, it was examined whether a more acidic *in vitro* environment would promote effective release of Gefitinib from its H-AFt cage. The investigations indicated that SKBR3 cells were unable to withstand pH < 7.0 environments for more than 72 h. However, at pH = 7.0, H-AFt-encapsulated-Gefitinib inhibited SKBR3 cell growth in a dose-dependent manner following 72 h exposure ($GI_{50} = 0.44 \pm 0.16 \times 10^{-6}$ M), exhibiting >3-fold enhanced potency, compared to pH 7.5. Clonogenic assays were performed to determine whether individual SKBR3 cells were able to survive challenge with Gefitinib or H-AFt-encapsulated-Gefitinib and subsequently form progeny colonies, indicative of tumor repopulation.[37] After 24 h exposure to agents followed by 13 d incubation with medium alone, H-AFt-encapsulated-Gefitinib demonstrated lower potency than Gefitinib (**Figure 4**). The survival fraction (SF) of cells treated with Gefitinib was 50.7% ± 1.5% (1×10^{-6} M) and 3.5% ± 1.0% (5×10^{-6} M) compared to control whereas SF of cells treated with H-AFt-encapsulated-Gefitinib was 71.8% ± 0.5% (1×10^{-6} M) and 34.4% ± 5.2% (5×10^{-6} M). However, following 14 d continuous exposure to both agents, no colonies could be detected. These results endorse the premise of sustained drug release from H-AFt as an efficient drug delivery system.

Release of Gefitinib from H-AFt into buffer was examined at pH 2, 4, and 7.5 over a period of 24 h by analyzing both the buffer and the solution retained within the dialysis bags. UV

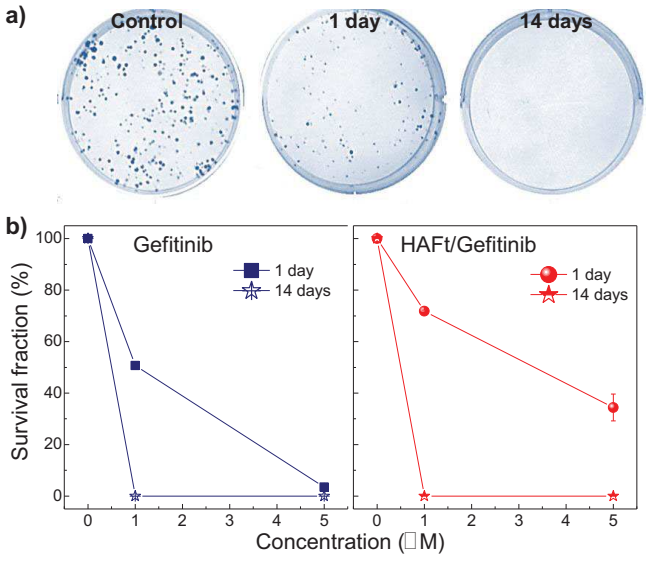

Figure 4. a) Photographs of SKBR3 colonies following treatment of cells with 5×10^{-6} M H-AFt-encapsulated-Gefitinib. b) Effect of Gefitinib and H-AFt-encapsulated-Gefitinib treatment on SKBR3 colony formation. Cells were exposed to drug for 14 d continuously or for 24 h only (1 d) followed by 13 d in medium alone. Mean and SD of three independent trials ($n = 3$ per trial).

spectrometry was adopted to compare Gefitinib release from H-AFt. At pH 2 the AFt cage completely disassembles, at pH 4 the AFt cage swells, separating the protein subunits and at pH 7.5 the AFt cage retains its assembled structure.[5] Rapid, cumulative diffusion of Gefitinib alone was observed at pH 7.5, reaching a plateau at 6 h. In comparison, at pH 2, 4, and 7.5, detection of Gefitinib released from H-AFt-encapsulated-Gefitinib indicates a slower cumulative release profile; progressively reduced drug was released from the AFt cage as pH increases (Section S4, Supporting Information). The most rapid cumulative release profile was observed at pH 2, consistent with the AFt cage disassembling and allowing Gefitinib release.

Analysis of residual buffer by flow cytometry (Section S4, Supporting Information) revealed only two negative populations at pH 2 and 4, exposing very low total fluorescence in the histograms relative to control. This implies that negligible amounts of Gefitinib were retained in the dialysis bags; after 24 h. However at pH 7.5, a small population positive for fluorescence was observed; indicating that some drug molecules remained encapsulated, confirming sustained release of Gefitinib from H-AFt at physiological pH levels.[36]

The *in vitro* results indicate that encapsulation of Gefitinib within an H-AFt cage could provide a facile route to targeted drug delivery and release in vivo. Recognition of H-AFt by TfR1 of cancer cells allows encapsulated cargo to be selectively internalized into cancer cells via TfR1 mediated endocytosis[3,4] and has successfully been utilized for targeted delivery of, e.g., MRI imaging agents. Although angiogenesis is enhanced in cancers[38] suggesting potential competition between endogenous ferritins and H-AFt uptake, a recent study demonstrated successful delivery of doxorubicin encapsulated in H-AFt to tumor sites and in vivo efficacy.[18] Thus, we envisage that the observed selective targeting and enhanced efficacy could be translated *in vivo* and merits further detailed studies.

In conclusion, successful encapsulation of Gefitinib within the H-AFt cavity, sustained release of cargo, and subsequent antitumor activity selectively in HER2 overexpressing breast carcinoma cells are shown. Utilizing the fluorescent property of Gefitinib, it was able to confirm intracellular localization of H-AFt-encapsulated-Gefitinib in SKBR3 cells. Potent, dose-dependent growth inhibition of cancer cells sensitive to EGFR inhibition was achieved and clonogenic assays further provided evidence of sustained Gefitinib release and significant *in vitro* anticancer activity of H-AFt-encapsulated-Gefitinib. H-AFt encapsulation can reduce off target toxicities of Gefitinib and diminish drug deposition in normal tissues. AFt encapsulation enhances the therapeutic efficacy of Gefitinib through passive targeted delivery and sustained release to tumor sites which demonstrates a successful nanoscale drug delivery system.

Experimental Section

Preparation and Characterization of H-AFt-Encapsulated-Gefitinib: Gefitinib (Cayman Chemical USA) was dissolved in DMSO:PBS (1:1 at pH 7.2) at a concentration of 1×10^{-3} M. 160×10^{-6} M synthetic human H-AFt expressed in *E. coli* was provided by Prof. N. R. Thomas. There were additional His- and Avidin-tags and also linker sequences in the provided H-AFt. This increases the size of H-AFt from 21 to ≈24 kDa. H-AFt was added to Gefitinib solution with 40-fold excess of drug, and was stirred overnight at 4 °C. The unencapsulated Gefitinib was removed by dialysis in 20×10^{-3} M Tris (pH 8.0) using a dialysis membrane (cut-off 8 kDa) for 48 h at 4 °C. Any impurities were removed by centrifugation (13 000 rpm, 12 min, 4 °C). The protein concentration of H-AFt was determined by Bradford assay.[39] The morphology was examined by TEM (JEOL 2100F at 200 kV). For sodium dodecyl sulfate (SDS)-PAGE, following denaturation (T = 95 °C for 5 min), 10 µL of H-AFt, H-AFt-encapsulated-Gefitinib and 5 µL of molecular marker (Thermo Scientific) were loaded onto a 4% stacking gel and resolved in a 12% resolving gel; samples were separated at 100 V for 2.5 h. The gel was stained overnight with 0.5% coomassie blue, followed by destaining with 50% methanol and 10% acetic acid, and imaged in an UVP BioDoc-It system.

Determining Encapsulation Efficiency (EE): Absorbance of serial dilutions of Gefitinib (from 250×10^{-6} to 0.5×10^{-6} M in DMSO) at 250 nm was analyzed using Perkin-Elmer Lambda 25 UV/vis Spectrometer and WinLab ver. 6.0.4.0738 and the Beer–Lambert law was used to quantify the encapsulated drug. The EE was estimated as a ratio between the concentration of the encapsulated drug and that used in synthesis.

Confirmation of Encapsulation of Gefitinib in H-AFt: H-AFt-encapsulated-Gefitinib solution was analyzed using an Astrios EQ flow cytometer (Beckman Coulter, Summit 6.2.3.1561) equipped with 488 and 355 nm lasers. Fluorescence emission was collected using a 405/30 band-pass filter.

Mass Spectrometry: For MALDI, H-AFt-encapsulated-Gefitinib (10 µL) was mixed with sinapic acid and 0.5 µL of the resulting solution was loaded onto a MALDI target sample plate. The plate was left to air dry for 5 min and was analyzed on the Bruker Ultraflex III spectrometer.

Cell Lines and Cell Culture: SKBR3 and MDA-MB-231 breast cancer cell lines (European Collection of Cell Cultures) were maintained in RPMI 1640 medium supplemented with 10% fetal bovine serum (FBS) at 37 °C in a humidified atmosphere containing 5% CO_2.

MTT Assay: Cells were seeded in 96 well plates (2.5×10^3 per well) for 24 h before treatment with Gefitinib, H-AFt-encapsulated-Gefitinib, and H-AFt. Following 72 h or 120 h exposure, MTT (3-(4,5-dimethylthiazol-2-yl)-2,5-diphenyltetrazolium bromide; 400 µg mL^{-1}) was added and plates were incubated for 2.5 h. Well supernatants were aspirated and formazan solubilized with 150 µL 100% DMSO. Absorbance at 550 nm was read on Perkin–Elmer plate reader. 1 M HCl was introduced into medium dropwise for MTT assays at pH 7.0.

Clonogenic Assay: SKBR3 cells (250 per well) were seeded into 6 well plates and allowed for 24 h to attach. Following 24 h treatment with Gefitinib and H-AFt-encapsulated-Gefitinib (1×10^{-6} and 5×10^{-6} M), in half of the wells test agent was replaced with 2 mL of fresh medium. Cells in the remaining wells were exposed to test agents for 14 d. Experiments were terminated when colonies of ≥ 50 cells were formed in control wells. Colonies were washed (PBS), fixed (methanol; 15 min), stained (0.5% methylene blue; 15 min) and counted. SF were calculated: SF = Plating efficiency of treated sample/Plating efficiency of control × 100%.[37]

Release of Gefitinib from H-AFt: Dialysis bags (cut-off 8 kDa) containing H-AFt-encapsulated-Gefitinib (100×10^{-6} M) and Gefitinib (100×10^{-6} M) diluted in 20×10^{-3} M Tris buffer (900 µL) were placed in separate beakers containing 20×10^{-3} M Tris buffer at pH 2, 4 or 7.5 at 37 °C, 5% CO_2. Released Gefitinib was quantified after 2, 6, 12, and 24 h by UV spectrophotometry at 250 nm. Gefitinib in the residual buffer within the dialysis bags was detected by Astrios EQ flow cytometry.

Cellular Uptake Studies: For confocal microscopy, SKBR3 and MDA-MB-231 (2×10^4) cells were seeded into 8 well coverslips and allowed to attach overnight. Following 24 h exposures with Gefitinib or H-AFt-encapsulated-Gefitinib (5×10^{-6} M), live imaging of cells was carried out using a Zeiss LSM 510 fluorescence microscope equipped with a UV laser of 351 nm excitation and LP385 emission filter. For flow cytometry studies, SKBR3 and MDA-MB-231 cells (2.5×10^5) were seeded in 6 well plates and allowed to attach overnight before 24 h exposure to Gefitinib or H-AFt-encapsulated-Gefitinib (5×10^{-6} M). Cells were washed and collected into FACS tubes. Using an Astrios EQ flow cytometer, 20 000 events were acquired and Gefitinib fluorescence was collected.

Statistical Analyses: All experiments were repeated ≥3 times and results are presented as means ± SD (Standard Deviation) or ± SE (Standard Error). Significant differences were defined as $P < 0.05$.

Supporting Information

Supporting Information is available from the Wiley Online Library or from the author.

Acknowledgements

This work was supported by Schlumberger Faculty for the Future (FFTF) program, NC3Rs/EPSRC. Authors thank Dr. David Onion, Dr. Michael W. Fay, and Melchior Cini for flow cytometry, TEM, and UV spectrometry expertise respectively.

Received: May 22, 2015
Revised: August 21, 2015
Published online: November 23, 2015

[1] K. S. Soppimatha, T. M. Aminabhavi, A. R. Kulkarnia, W. E. Rudzinskib, *J. Control. Release.* **2001**, *70*, 1.
[2] W. H. De Jong, P. J. Borm, *Int. J. Nanomedicine.* **2008**, *3*, 133.
[3] F. Danhier, O. Feron, V. Préat, *J. Control. Release* **2010**, *148*, 135.
[4] T. R. Daniels, E. Bernabeu, J. A. Rodríguez, S. Patel, M. Kozman, D. A. Chiappetta, E. Holler, J. Y. Ljubimova, G. Helguera, M. L. Penichet, *Biochimica Biophysica Acta* **2012**, *1820*, 291.
[5] A. Ma-Ham, H. Wu, J. Wang, X. Kang, Y. Zhang, Y. Lin, *J. Mater. Chem* **2011**, *21*, 8700.
[6] Z. Yang, X. Wang, H. Diao, J. Zhang, H. Li, H. Sun, Z. Guo, *Chem. Commun.* **2007**, *33*, 3409.
[7] A. Ma-Ham, Z. Tang, H. Wu, J. Wang, Y. Lin, *Small* **2009**, *5*, 1706.
[8] Z. Heger, S. Skalickova, O. Zitka, V. Adam, R. Kizek. *Nanomedicine* **2014**, *9*, 2233.
[9] L. Zhang, L. Laug, W. Münchgesang, E. Pippel, U. Gösele, M. Brandsch, M. Knez, *Nano Lett.* **2010**, *10*, 219.
[10] L. Li, C. J. Fang, J. C. Ryan, E. C. Niemi, J. A. Lebrón, P. J. Björkman, H. Arase, F. M. Torti, S. V. Torti, M. C. Nakamura, W. E. Seaman, *Proc. Natl. Acad. Sci. USA* **2010**, *107*, 3505.
[11] L. Zhang, W. Fischer, E. Pippel, G. Hause, M. Brandsch, M. Knez, *Small* **2011**, *7*, 1538.
[12] S. V. Torti, F. M. Torti, *Nat. Rev. Cancer* **2013**, *13*, 342.
[13] A. Schroeder, D. A. Heller, M. M. Winslow, J. E. Dahlman, G. W. Pratt, R. Langer, T. Jacks, D. G. Anderson, *Nat. Rev. Cancer* **2012**, *12*, 39.
[14] Z. Zhen, W. Tang, H. Chen, X. Lin, T. Todd, G. Wang, T. Cowger, X. Chen, J. Xie, *ACS Nano.* **2013**, *7*, 4830.
[15] M. A. Kilic, E. Ozlu, S. Calis, *J. Biomed. Nanotechnol.* **2012**, *8*, 508.
[16] S. G. Crich, B. Bussolati, L. Tei, C. Grange, G. Esposito, S. Lanzardo, G. Camussi, S. Aime, *Cancer Res.* **2006**, *66*, 9196.
[17] K. Fan, C. Cao, Y. Pan, D. Lu, D. Yang, J. Feng, L. Song, M. Liang, X. Yan, *Nat. Nanotechnol.* **2012**, *7*, 459.
[18] M. Liang, K. Fan, M. Zhou, D. Duan, J. Zheng, D. Yang, J. Feng, X. Yan, *Proc. Natl. Acad. Sci. USA* **2014**, *111*, 14900.
[19] M. H. Cohen, G. A. Williams , R. Sridhara, G. Chen, W. D. McGuinn Jr., D. Morse, S. Abraham, A. Rahman, C. Liang, R. Lostritto, A. Baird, R. Pazdur, *Clin. Cancer Res.* **2004**, *10*, 1212.
[20] M. D. Marmor, K. B. Skaria, Y. Yarden, *Int. J. Radiat. Oncol.* **2004**, *58*, 903.
[21] Y. Yarden, G. Pines, *Nat. Rev. Cancer* **2012**, *12*, 553.
[22] S. A. Hurvitz, Y. Hu, N. O'Brien, R. S. Finn, *Cancer Treat. Rev.* **2013**, *39*, 219.
[23] K. Subik, J. Lee, L. Baxter, T. Strzepek, D. Costello, P. Crowley, L. Xing, M. Hung, T. Bonfiglio, D. G. Hicks, P. Tang, *Breast Cancer* **2010**, *4*, 35.
[24] M. Campiglio, A. Locatelli, C. Olgiati, N. Normanno, G. Somenzi, L. Viganò, M. Fumagalli, S. Menard, L. Gianni, *J. Cell. Phys.* **2004**, *198*, 259.
[25] F. R. Hirsch, M. Varella-Garcia, F. Cappuzzo, *Oncogene* **2009**, *28*, S32.
[26] A. Haringhuizen, H. van Tinteren, H. F. R. Vaessen, P. Baas, N. van Zandwijk, *Ann. Oncol.* **2004**, *15*, 786.
[27] X. Zhou, B. Yung, Y. Huang, H. Li, X. Hu, G. Xiang, R. J. Lee, *Anticancer Res.* **2012**, *32*, 2919.
[28] Y. Shi, C. Su, W. Cui, H. Li, L. Liu, B. Feng, M. Liu, R. Su, L. Zhao, *J. Nanobiotechnol.* **2014**, *12*, 43.
[29] A. A. Pawar, D. Chen, C. Venkataraman, *Int. J. Pharm.* **2012**, *430*, 228.
[30] S. P. Gautam, A. K. Gupta, S. Agrawal, S. Sureka, *Int. J. Pharm. Pharm. Sci.* **2012**, *4*, 77.
[31] B. J. Trummer, V. Iyer, S. V. Balu-Iyer, R. O'Connor, R. M. Straubinger, *J. Pharm. Sci.* **2012**, *101*, 2763.
[32] D. S. Hirsch, Y. Shen, W. J. Wu, *Cancer Res.* **2006**, *66*, 3523.
[33] M. Kawamoto, T. Horibe, M. Kohno, K. Kawakami, *BMC Cancer* **2011**, *11*, 2.
[34] Y. Zheng, B. Yu, W. Weecharangsan, L. Piao, M. Darby, Y. Mao, R. Koynova, X. Yang, H. Li, S. Xu, L. J. Lee, Y. Sugimoto, R. W. Brueggemeier, R. J. Lee, *Int. J. Pharm.* **2010**, *390*, 234.
[35] A. A. Alkhateeb, B. Han, J. R. Connor, *Breast Cancer Res. Treat.* **2013**, *137*, 733.
[36] E. S. Lee, Y. H. Bae, *J. Control. Release* **2008**, *132*, 164.
[37] N. A. P. Franken, H. M. Rodermond, J. Stap, J. Haveman, C. van Bree, *Nat. Protoc.* **2006**, *1*, 2315.
[38] L. G. Coffman, D. Parsonage, R. D'Agostino Jr., F. M. Torti, S. V. Torti, *Proc. Natl. Acad. Sci. USA* **2009**, *106*, 570.
[39] M. M. Bradford, *Anal. Biochem.* **1976**, *72*, 248.

